Defense Technical Information Center Compilation Part Notice

ADP013655

TITLE: Large Eddy Simulation of Supersonic Compression Corner Using ENO Scheme

DISTRIBUTION: Approved for public release, distribution unlimited

This paper is part of the following report:

TITLE: DNS/LES Progress and Challenges. Proceedings of the Third AFOSR International Conference on DNS/LES

To order the complete compilation report, use: ADA412801

The following component part numbers comprise the compilation report:
ADP013620 thru ADP013707

LARGE EDDY SIMULATION OF SUPERSONIC COMPRESSION CORNER USING ENO SCHEME

HONG YAN, DOYLE KNIGHT
Department of Mechanical and Aerospace Engineering
Rutgers – The State University of New Jersey
Piscataway, N.J. 08854-8058, USA

AND

ALEXANDER A. ZHELTOVODOV
Institute of Theoretical and Applied Mechanics
Russian Academy of Sciences - Siberian Branch
Novosibirsk 630090, Russia

1. Abstract

A Large Eddy Simulation of a 25° compression corner at $M = 2.88$ and $Re_\delta = 2 \times 10^4$ is performed using an Essentially Non Oscillatory (ENO) scheme. The Favre filtered compressible Navier-Stokes equations are solved using a Monotone Integrated Large Eddy Simulation (MILES) technique on an unstructured grid of tetrahedral cells. The mean flow variables and turbulent shear stress at the incoming flow are in good agreement with experiment and DNS. The separation length scaled by the characteristic scale [27, 31] shows agreement with the experiment. No pronounced pressure plateau is observed compared with experiment at higher Reynolds number.

2. Introduction

Supersonic flow over a compression corner is a classic problem embodying all the difficulties of viscous/inviscid interactions, compressibility and turbulence. A full understanding of this configuration is important for efficient aerodynamic and propulsion design. An extensive effort [1, 3, 4, 6, 7, 8, 10, 11, 15, 16, 17, 18, 20, 21, 22, 24, 25, 26, 27, 29, 30, 31, 32] has been focused on the study of this flow. However, traditional RANS meth-

ods have not accurately predicted the heat transfer and skin friction coefficient[3, 4, 10, 18, 29, 30] in cases with large flow separation. In addition, the scaled seperation length proposed in [27, 31] shows a significant deviation from the experimental range in Fig. 1. A Very Large Eddy Simulation by Hunt [11] for a 24° Mach 2.8 compression corner at $Re_\delta = 10^6$ revealed that the size of the separation bubble correlates strongly with the shock wave position. A DNS of 18° Mach 3 compression corner at $Re_\theta = 1685$ implemented by Adams [1] indicated the effect of compressibility on the turbulence structure in the interaction area. Rizzetta *et al.* [16, 17] performed a DNS and LES of 18° compression corner and made full comparison with DNS results by Adams [1].

This paper implements an ENO scheme for a 25° compression corner at Mach 2.88 and $Re_\delta = 2 \times 10^4$ to assess the capability of LES to accurately predict the turbulence characteristics.

3. Methodology

The Monotone Integrated Large Eddy Simulation technique [2] is used to solve the Favre-filtered compressible Navier-Stokes equations. The inviscid fluxes are computed using the second order Godunov's method and the viscous fluxes and heat transfer are obtained by application of Gauss' Theorem to each face. An ENO scheme has been developed for the unstructured grid. Our LES code is parallelized using domain decomposition in spanwise direction with Portable Message Passing Interface Model Implementation `Mpich`. The details are presented in [5, 14].

Allowing x, y and z to denote the streamwise, transverse and spanwise directions, respectively, the computational domain is $L_x = 16.0\delta$, $L_y = 3.4\delta$, and $L_z = 1.925\delta$. The grid consists of $213 \times 35 \times 57$ nodes in the x, y and z directions, respectively. The reference quantities for nondimensionalization are length δ (the incoming boundary layer thickness), velocity U_∞, density ρ_∞, static temperature T_∞ and molecular viscosity μ_∞ (where the subscript ∞ denotes the freestream conditions upstream of the compression corner). The tetrahedral grid is employed and stretched in the y direction with a spacing of 0.008δ at the wall and the stretching factor of 1.154. The grid is concentrated around the compression corner. The details of the grid are shown in Table 1, wherein $\Delta y^+ = \Delta y/\eta$ with the inner length scale $\eta = \nu_w/u_\tau$ (ν_w is the kinematic viscosity at the wall, $u_\tau = \sqrt{\tau_w/\rho_w}$ is the friction velocity, τ_w is the wall shear stress and ρ_w is the density at the wall). The theoretical values of u_τ and ν_w are obtained from the combined Law of the Wall and Wake evaluated at $y = \delta$ and the power law of the relationship between temperature and kinematic viscosity, respectively.

TABLE 1. Details of Grids

Name	Mach	Δx^+	Δy^+ at the wall	Δz^+	$\Delta x/\delta$	$\Delta y/\delta$ at $y = \delta$	$\Delta z/\delta$	Tetras
Theoretical value	2.88	24	1.9	8.1	0.1	0.14	0.034	
LES	2.88	20.9	1.67	7.1	0.1	0.14	0.034	2,018,240

The inflow condition is obtained from a separate flat plate boundary layer computation. The non-slip boundary condition is used to the adiabatic wall. All the flow variables shown in the figures are averaged in time and the spanwise direction. The time averaging period is set to three times the flow-through time, where one flow-through time is defined as the time for the freestream flow to traverse the computational domain. The details are presented in [21].

4. Results

The oncoming flow characteristics are illustrated by the mean flow variables in Fig. 3 and Fig. 4 and the Reynolds shear stress in Fig. 5. The comparisons with experiments [28] and DNS show good agreement.

Fig. 2 shows the pressure contour distribution at $x - y$ plane of $z = 1.0\delta$. A strong separation and attachment shock wave is formed at the compression corner leading to the higher pressure level after the shock. The strong adverse pressure gradient causes the skin friction coefficient to decrease dramatically and the flow separates. Downstream of the corner, the overall increase in pressure and the decrease in Mach number cause the skin friction coefficient to recover.

The computational results are shown in Fig. 6–Fig. 8 along with experimental data. The skin friction coefficient in Fig. 6 is compared with the experiment at higher Reynolds number of $Re_\delta = 63560$. According to the Law of the Wall and Wake, the friction velocity is decreased with the increase in Reynolds number, leading to the higher skin friction coefficient in the computation. The time and spanwise averaged surface pressure profile along the streamwise direction is compared with experiment at higher Reynolds number in Fig. 7 and the pressure plateau is not observed. The difference between the predicted and experimental surface pressure profile may be attributable to the difference in Reynolds number.

The effect of Reynolds number on the separation length is plotted in

Fig. 8. In this figure, the separation length is measured by connecting the separation and attachment points at which the time and spanwise averaged skin friction coefficients go to zero and then scaled by the characteristic length (L_c) proposed by Zheltovodov and Schuelein [27, 31]

$$L_c = \delta(p_2/p_{pl})^{3.1}/M_\infty^3 \tag{1}$$

where δ is the incoming boundary layer thickness, p_2 is the pressure after the shock in inviscid flow, p_{pl} is the plateau pressure obtained by the empirical formula $p_{pl} = p_\infty(0.5M_\infty + 1)$ [33] and M_∞ is the Mach number in the uniform flow. Some LES and DNS results by other researchers are also plotted in Fig. 8 for comparison. Our LES successfully predicts the consistent trend with the experiment.

5. Conclusion

A 25° supersonic compression corner at Mach 2.88 and $Re_\delta = 2 \times 10^4$ has been simulated using an Essentially Non Oscillatory (ENO) scheme. The mean quantities in the incoming equilibrium flow show good agreement with experiment. The separation length is consistent with the extrapolated experimental trend. Computations at higher Reynolds number are in progress.

6. Acknowledgement

The research is supported by AFOSR under grant No. F49620-99-1-0008 monitored by Drs. Robert Herklotz, Len Sakell, John Schmisseur and Steve Walker.

References

1. Adams, N. A. (2000) Direct Simulation of the Turbulent Boundary Layer along a Compression Ramp at $M = 3$ and $Re_\theta = 1685$, *J. Fluid Mech.*, **Vol. 420, pp. 47–83**
2. Boris, J., Grinstein, F., Oran, E. and Kolbe R. (1992) New Insights into Large Eddy Simulation, *Fluid Dynamics Research*, **Vol. 10, pp. 199–228**
3. Borisov, A. V., Zheltovodov, A. A., Badekas, D. and Narayanswami, N. (1995) Computational Study of Supersonic Turbulent Separated Flows in the vicinity of Inclined Steps, *J. Applied Mechanics and Technical Physics*, **Vol. 36, No. 3, pp. 68–80** (in Russian)
4. Borisov, A. V., Zheltovodov, A. A., Maksimov, A. I., Fedorova, N. N. and Shpak, S. I. (1996) Verification of Turbulence Models and Computational Methods of Supersonic Separated Flows, *8th International Conference on Methods of Aerophysical Research, Institute of Theoretical and Applied Mechanics, Russian Academy of Sciences, Novosibirsk, Russia*
5. Chernyavsky, B., Yan, H. and Knight, D. (2001) Analyses of Some Numerical Problems in LES, *AIAA Paper 2001-0436*

6. Dolling, D. S. and Murphy, M. T. (1983) Unsteadiness of the Separation Shock Wave Structure in a Supersonic Compression Ramp Flowfield, *AIAA J.*, **Vol. 23, No. 12, pp. 1628–1634**
7. Dolling, D. S. (1983) Fluctuating Loads in Shock Wave/Turbulent Boundary Layer Interaction: Tutorial and Update, *AIAA Paper 93-0284*
8. Erengil, M. E. and Dolling, D. S. (1991) Correlation of Separation Shock Motion with Pressure Fluctuations in the Incoming Boundary Layer, *AIAA J.*, **Vol. 29, No. 11, pp. 1868–1877**
9. Horstman, C C and Hung, C M. (1977) Reynolds Number Effects on Shock-Wave Turbulent Boundary-Layer Interaction - A Comparison of Numerical and Experimental Results, *AIAA paper 77-42*
10. Horstman, C. C. and Zheltovodov, A. A. (1994) Numerical Simulation of Shock Waves/Expansion Fans – Turbulent Boundary Layer Interaction, *Proc: Int. Conference on the Methods of Aerophysical Research, Novosibirsk, Part II*, **pp. 118–125**
11. Hunt, D. (1995) A Very Large Eddy Simulation of an Unsteady Shock Wave/Turbulent Boundary Layer Interaction, *AIAA Paper 95-2212*
12. Konrad, W. and Smits, W. (1998) Turbulence Measurements in a Three-Dimensional Boundary Layer in Supersonic Flow, *J. Fluid Mech.*, **Vol. 372, pp. 1–23**
13. Muck, K., Spina, E. and Smits, A. (1984) Compilation of Turbulence Data for an 8 degree Compression Corner at Mach 2.9, *Tech. Rep. Report MAE-1642, Princeton University*
14. Okong'o, N. and Knight, D. (1998) Compressible Large Eddy Simulation Using Unstructured Grids: Channel and Boundary Layer Flows, *AIAA Paper 98-3315*
15. Ong, C. and Knight, D. (1987) Hybrid MacCormack and Implicit Beam-Warming Algorithms for a Supersonic Compression Corner, *AIAA J.*, **Vol. 25, No. 3, pp. 401–407**
16. Rizzetta, D. P., Visbal, M. R. and Gaitonde, D. V. (2000) Direct Numerical and Large-Eddy Simulation of Supersonic Flows by a High-Order Method, *AIAA Paper 2000-2408*
17. Rizzeta, D. and Visbal, M. (2001) Large-Eddy Simulation of Supersonic Compression Ramp Flows, *AIAA Paper 2001-2858*
18. Settles, G. S., Fitzpatrick, T. J. and Bogdonoff, S. M. (1979) Detailed Study of Attached and Separated Compression-corner Flowfields in High Reynolds Number Supersonic Flow, *AIAA J.*, **Vol. 17, pp. 579–585**
19. Shang, J S and Hankey Jr, W L. (1975) Numerical Solution for Supersonic Turbulent Flow over a Compression Corner, *AIAA J.*, **Vol. 13, No. 10, pp. 1368–1374**
20. Unalmis, O. H. and Dolling D. S. (1994) Decay of Wall Pressure Field and Structure of a Mach 5 Adiabatic Turbulent boundary Layer, *AIAA Paper 94-2363*
21. Urbin, G., Knight, D. and Zheltovodov, A. A. (1999) Compressible Large Eddy Simulation using Unstructured Grid: Supersonic Turbulent Boundary Layer and Compression Corner, *AIAA Paper 99-0427*
22. Urbin, G., Knight, D. and Zheltovodov, A. A. (2000) Large Eddy Simulation of a Supersonic Compression Corner Part I, *AIAA Paper 2000-0398*
23. Visbal, M and Knight, D. (1984) The Baldwin-Lomax Turbulence Model for Two-Dimensional Shock-Wave/Boundary-Layer Interactions, *AIAA J.*,**Vol. 22, No. 7, pp. 921–928**
24. Wilcox, D. C. (1990) Supersonic Compression Corner Applications of a Multiscale Model for Turbulent Flows, *AIAA J.*, **Vol. 28, No. 7, pp. 1194–1198**
25. Yan, H., Urbin, G., Knight, D. and Zheltovodov, A. A. (2000) Compressible Large Eddy Simulation Using Unstructured Grid: Supersonic Boundary Layer and Compression Ramps, *10th International Conference on Methods of Aerophysical Research, Institute of Theoretical and Applied Mechanics, Russian Academy of Sciences, Novosibirsk, Russia*
26. Zheltovodov, A. A. and Yakovolev, V. (1986) Stages of Development, Gas Dy-

namic Structure and Turbulence Characteristics of Turbulent Compressible Separated Flows in the Vicinity of 2-D Obstacles, *Preprint No 27-86, Institute of Theoretical and Applied Mechanics, USSR Academy of Sciences* (in Russian)

27. Zheltovodov, A. A. and Schuelein, E. (1987) The Peculiarities of Turbulent Separation Development in Disturbed Boundary Layers, *Modeling in Mechanics*,**Vol. 2, No. 1, pp. 53–58** (in Russian)
28. Zheltovodov, A. A., Trofimov, V. M., Schuelein, E. and Yakovlev, V. N. (1990) An Experimental Documentation of Supersonic Turbulent Flows in the Vicinity of Sloping Forward- and Backward-Facing Ramps, *Rep No 2030, Institute of Theoretical and Applied Mechanics, USSR Academy of Sciences*
29. Zheltovodov, A. A., Borisov, A. V., Knight, D. D., Horstman, C. C. and Settles, G. S. (1992) The Possibilities of Numerical Simulation of Shock Waves/Boundary Layer Interaction in Supersonic and Hypersonic FLows, *Proc: Int. Conference on the Methods of Aerophysical Research, Novosibirsk, Part I*, **pp. 164–170**
30. Zheltovodov, A. A. and Horstman, C. C. (1993) Experimental and Numerical Investitgation of 2-D Expansion/Shock Wave – Turbulent Boundary Layer Interaction, *Preprint No 2-93, Institute of Theoretical and Applied Mechanics, Russian Academy of Sciences, Novosibirsk*
31. Zheltovodov, A. A., Schuelein, E. and Horstman, C. C. (1993) Development of Separation in the Region where a Shock Interacts with a Turbulent Boundary Layer Perturbed by Rarefaction Waves, *J. Applied Mechanics and Technical Physics*, **Vol. 34, No. 3, pp. 58–68**
32. Zheltovodov, A. A. (1996) Shock Waves / Turbulent Boundary Layer Interaction - Fundamental Studies and Applications, *AIAA Paper 96-1977*
33. Zukoski, E. E. (1967) Turbulent Boundary Layer Separation in front of a Forwrad Facing Step, *AIAA J.*, **Vol. 5, No. 10, pp. 1746–1753**

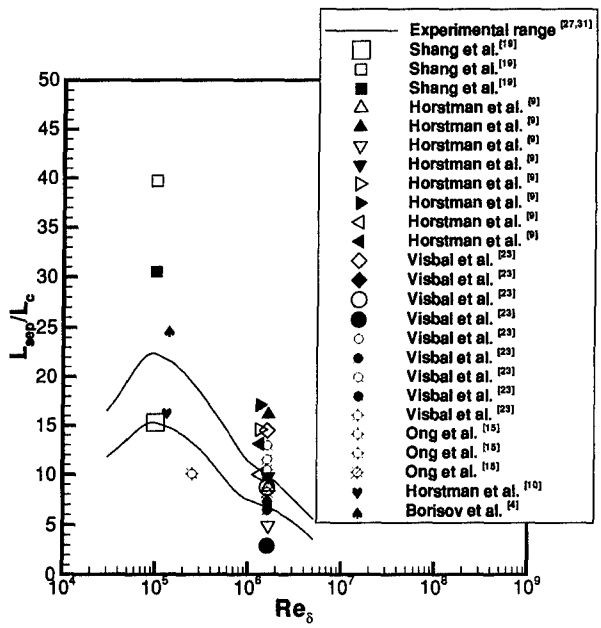

Figure 1. Separation length for RANS

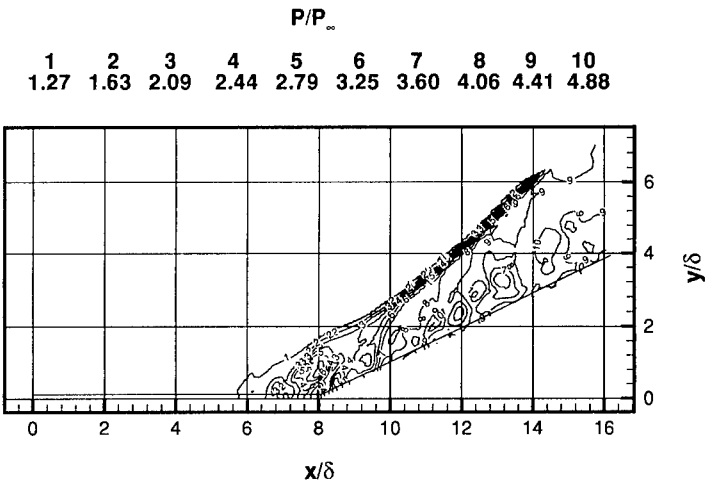

Figure 2. Instantaneous pressure contour

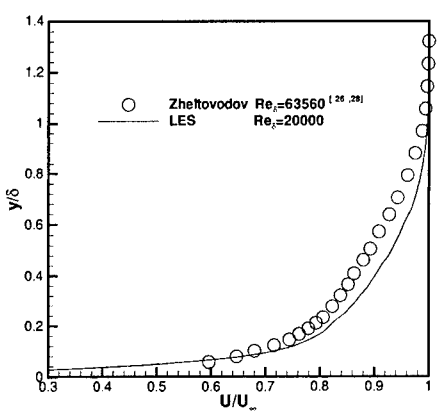

Figure 3. Mean streamwise velocity

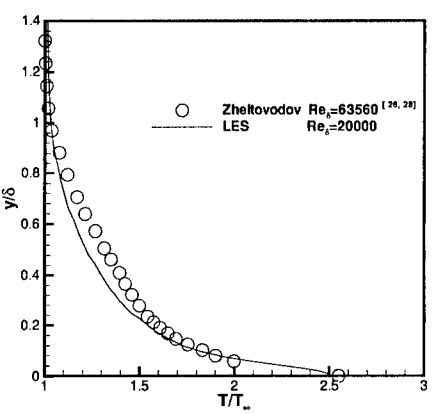

Figure 4. Mean temperature

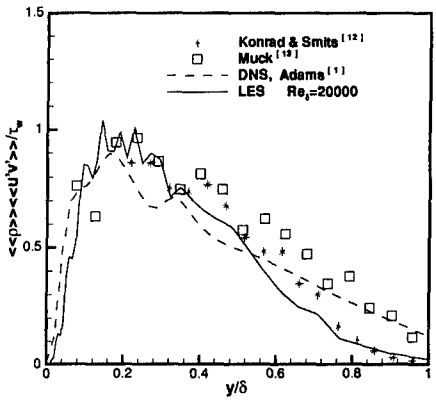

Figure 5. Reynolds shear stress

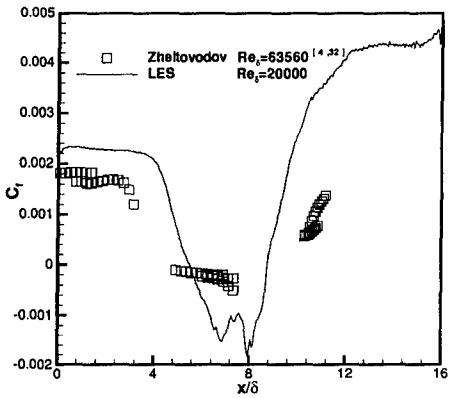

Figure 6. Skin friction coefficient

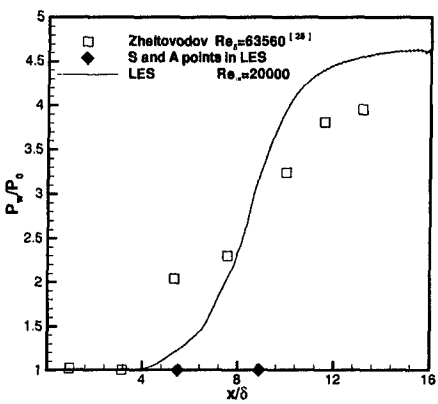

Figure 7. Surface wall pressure

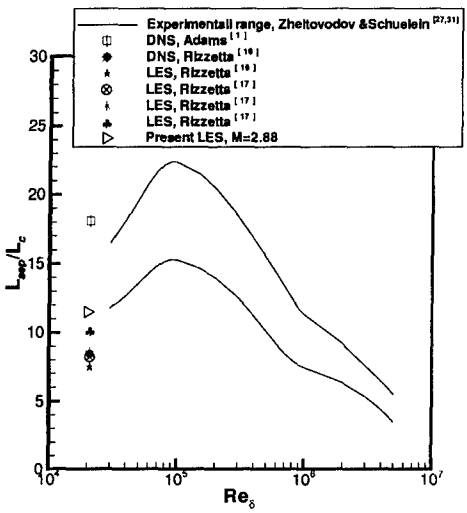

Figure 8. Separation length for LES and DNS